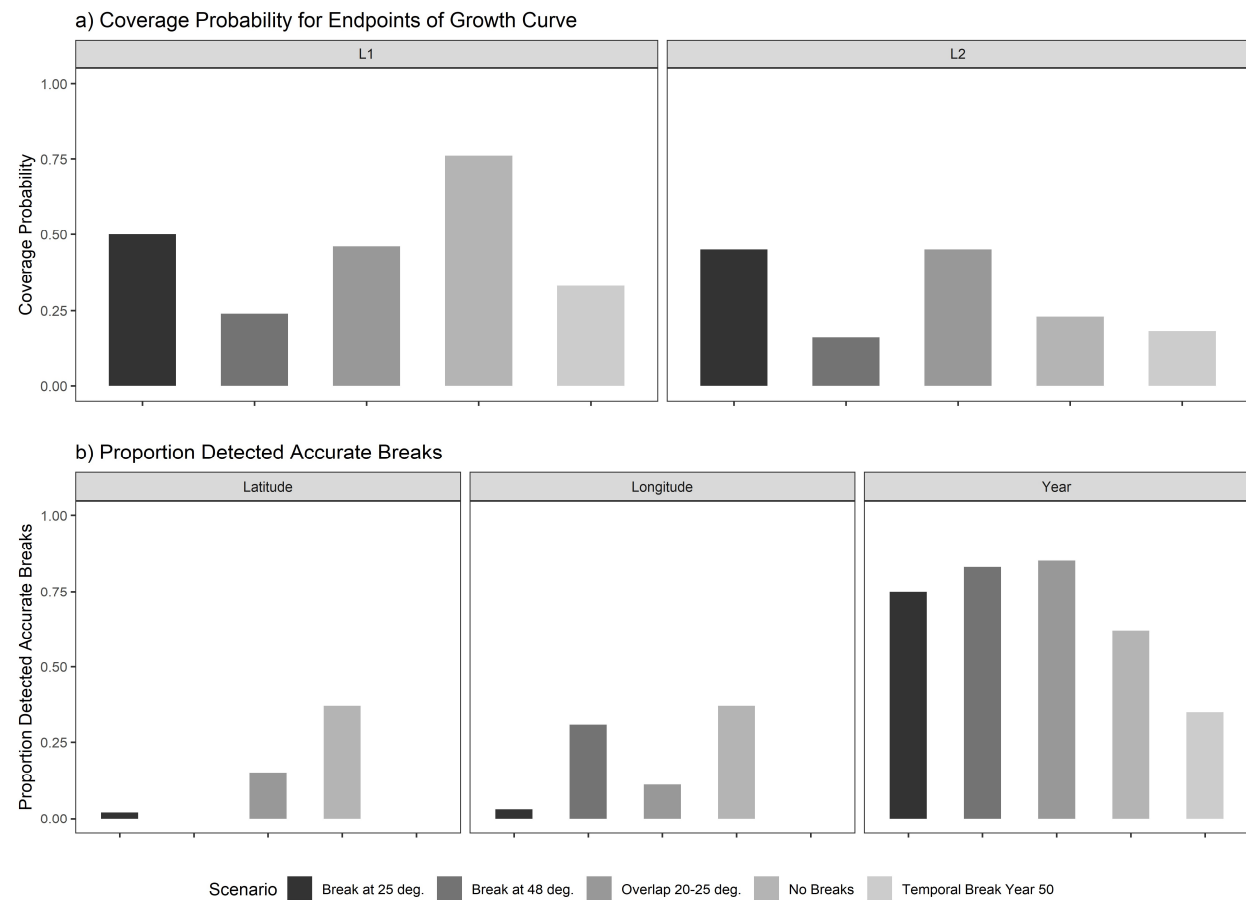


1    *Supplementary Material -- Details of the Individual-Based Model (IBM)*

2    This document describes the equations and assumptions used to generate the length-at-age datasets used in  
3    the simulation testing component of this study. The first section describes the generation of the observed data,  
4    and the second section details further how spatial variation in fish size at age is introduced. Table A1 provides  
5    parameter values used in the study.

6

7    *A.1 STARS Method Results*



8  
9    Figure A1. Using the STARS method (Rodionov, 2004) a) coverage probabilities for the endpoints of the  
10   growth curve,  $L_1$  (left) and  $L_2$  (right), and b) proportion of 100 simulations for each spatial scenario wherein  
11   the correct latitudinal breaks (left), or longitudinal breaks (center) or yearly break (right) were detected.

12   **Commentary on comparison of simulation study and STARS method**

13  
14   We observed decreased ability of the method to detect breakpoints near the edge of the range, with a true  
15   break at  $48^\circ$  inconsistently being assigned between  $46^\circ$  and  $50^\circ$ . This outcome, and the resultant low coverage  
16   probabilities for parameters  $L_1$  and  $L_2$  for this scenario were likely due to the smaller number of samples  
17   present in the ‘edge’ of the simulated space, and contrast in length-at-age between the two regions, which  
18   rendered estimates of aggregated data uninformative. This suggests that fishery scientists and managers may  
19   need alternative tools to detect and appropriately consider variation in growth at the extremes of a stock’s

spatial domain, or occurring at present. Such breakdown of detection methods at the margins of a series (at the edges of a study region, or at the end of a time-series) has been documented in Rodionov (2004), who developed a method using sequential *t*-tests (STARS) to perform edge-case detection, and applied it to detect ecosystem regime shifts in the Bering Sea (Rodionov and Overland, 2005). The *t*-test approach can be tuned by the researcher to control the level of significance that determines a regime shift (or breakpoint), presenting the same challenge of spurious and/or missed detections depending on the sensitivity of the statistical test applied. Our comparison with the STARS method demonstrated that the GAM-based method performs better at accurately detecting spatial-temporal breakpoints, except for scenarios where the break occurs at the edge of the study system, which was expected. In terms of the coverage probabilities, both methods had a slightly reduced ability to correctly estimate  $L_2$ , with the STARS method performing slightly better. We believe this outcome is due to two interacting processes: the GAM-based method's sensitivity to temporal variation, and bias in parameter estimates due to reduced sample sizes at high ages. The GAM appeared to be more sensitive to temporal signals in the datasets, and though it correctly detected (or correctly failed to detect) a temporal breakpoint in the majority of datasets, when it mis-detected a year break it did so seemingly at random, thus splitting the dataset into arbitrary groups and leading to lower accuracy of estimation. This phenomenon was more pronounced for  $L_2$  since  $L_2$  relies on fish near the terminal age, of which there are typically fewer, and can lead to bias in the resultant estimate when the already-small sample of fish at age  $a_2$  is split further due to spurious year detections. Indeed, for all scenarios besides Scenarios 1 and 4 (no breaks and break-at-edge), the margin by which  $L_2$  was missed was greater in simulations that mis-detected the year break (see Supplementary Material, Table A4). For assessment methods that estimate VBGF growth parameters within the assessment model, this low-data/low-accuracy issue for the terminal length may induce greater uncertainty (e.g., the need for priors with higher standard deviations) until targeted survey sampling can improve precision in less-represented management areas.

43

44 *A.1 Generation of age-length data*

45 The IBM is designed to mimic individual variation in growth for an unexploited fishery. The model runs for  
 46 100 years. Generally, all fish within each simulation are subject to the same baseline life history parameters,  
 47 with three growth “regimes” (defined by distinct values for the parameters of the growth equation, see below)  
 48 assigned spatial ranges accordingly (see Section A.1.4 Assigning spatio-temporal variation, below). Here we  
 49 detail the growth component of the IBM, code to execute the simulations is available here:  
 50 [https://github.com/mkapur/sab-growth/blob/master/IBM\\_master.R](https://github.com/mkapur/sab-growth/blob/master/IBM_master.R)

51

52

53 *A.1.1. Growth*

54 The growth module of the IBM is a von Bertalanffy growth function parameterized in terms of  $L_1$  and  $L_2$ :

$$55 L_{\infty} = L_1 + \frac{(L_2 - L_1)}{1 - e^{(-k \times (a_2 - a_1))}} \quad \text{App. Equation 1}$$

56 where  $L_{1,2}$  represents the lengths of a fish at ages  $a_{1,2}$ , and  $k$  is the growth coefficient. The size of individual  
 57  $i$  at age  $a$  is defined by its length in the previous year and a growth increment  $I$  that is lognormal:

$$58 L_{i,a} = \begin{cases} L_1 \varepsilon & \text{for } a = 1 \\ L_{i,a-1} + (I_{i,a-1}) \varepsilon_{i,a} & \text{for } a > 1 \end{cases} \quad \text{App. Equation 2}$$

59 where  $I_{i,a} = (L_{\infty} - L_{i,a})(1 - e^K)$  and  $\varepsilon_{i,a} \sim \exp\left(N(0, \sigma_{\varepsilon}) - \frac{\sigma_{\varepsilon}^2}{2}\right)$ ;  $\sigma_{\varepsilon} = 0.025$  for all ages and growth  
 60 regimes (Table A1). The value for  $\sigma_{\varepsilon}$  was selected so that the growth increments were similar to those for  
 61 sablefish.

62 *A.1.2 Survival*

63 The composition of the fishery during year  $y$  includes all surviving fish from recruitment to a maximum age  
 64 (represented here as a plus group  $a_2^+$ ). After recruitment, all fish are subject to mortality, which consists only  
 65 of natural mortality ( $M$ ; set to  $0.25\text{yr}^{-1}$  for all ages and years) as there is no fishery, thus fishing mortality  
 66 (typically denoted  $F$ ) and selectivity are ignored. Because no fishing pressure nor selectivity acted upon the  
 67 simulated population, we are unconcerned about variation in growth that can either be engendered (over time)  
 68 or misrepresented by differences in selectivity<sup>1</sup>. Whether an individual survives the year is simulated by  
 69 randomly drawing a number  $u$  from  $U[0,1]$  and allowing the individual to survive if this number is less than  
 70  $\exp(-M)$ , i.e.:

71

$$72 S_{i,y,a} = \begin{cases} 1 & \text{if } u_i < e^{-M} \\ 0 & \text{if } u_i > e^{-M} \end{cases} \quad \text{for } 0 \leq a \leq a_2^+ \quad \text{App. Equation 3}$$

73 where  $S_{i,y,a}$  is a value to indicate whether individual  $i$  is alive (1) or dead (0) during year  $y$  when it would be  
 74 of age  $a$ .

---

<sup>1</sup> This was not assumed, however, for the sablefish application.

75 We initialized the population in year zero at equilibrium as follows. The number of fish in the system is scaled  
 76 by  $R_0$ , or the expected number of recruits for an unfished population. For computational efficiency we set  
 77  $R_0=12$  (see sensitivities on sample size in later sections). Numbers at age are rounded to the nearest integer.  
 78

$$79 N_{y=0,a} = \begin{cases} R_0 & \text{for } a = 0 \\ N_{0,a-1}e^{-M} & \text{for } 1 \leq a < a_2^+ \\ \frac{N_{0,a_2-1}}{1-e^{-M}} & \text{for } a = a_2^+ \end{cases} \quad \text{App. Equation 4}$$

80 Lengths and weights for each individual in year 0 are calculated as in App. Equations 1 and 2. The starting  
 81 stock spawning biomass ( $SSB_0$ ) is calculated using the sum of expected weights, maturities, and numbers of  
 82 individuals at all ages in year 0. Maturity at age  $x_{0,a}$  is given by App. Equation 7a:

$$84 SSB_0 = \sum_1^{a_2^+} N_{0,a} W_{0,a} x_{0,a} \quad \text{App. Equation 5}$$

85 Otherwise, the total number of individuals of age  $a$  in the population in simulation year  $y$  (where  $y > 0$ ) is  
 86 given by:

$$88 N_{y,a} = \sum_1^i S_{i,y,a} \quad \text{App. Equation 6}$$

89

#### 90 A.1.3 Recruitment

91 Recruitment in the IBM is governed by a Beverton-Holt stock-recruitment function (Beverton and Holt,  
 92 1957), and a size-based maturity ogive that determines the probability of individual  $i$  maturing in a given year  
 93  $y$ ,  $p_{i,y}$ . The maturity ogives were fixed for all regimes, with  $L_{50}$  (the length at 50% maturity) at 75 cm, and  
 94 the slope of the ogive at -0.1034. The probability of an individual maturing in a given year  $p_{i,y}$  is conditional  
 95 on the probability in the current and previous year of being mature  $x_{i,y}$ , and  $x_{i,y-1}$ , which is then converted  
 96 to  $m_{i,y}$  (0 for immature; 1 for mature) by randomly drawing a number  $u_i$  from  $U[0,1]$  and defining the animal  
 97 as mature if  $u_i$  is less than  $p_{i,y}$ .

98 Recruitment in a given year  $R_y$  is the sum of the sum of empirical weights of each individual that is mature  
 99 in that year, which is governed by a deterministic exponential length-weight relationship (Figure A2). The  
 100 parameters of this relationship were the same for all regimes. Recruitment is subject to variation via a bias-  
 101 corrected lognormal recruitment deviation  $\partial_{r,y}$ .

102

$$103 \begin{aligned} x_{i,y} &= \frac{1}{1+\exp[-0.1034(L_{i,y}-L_{50})]} \\ p_{i,y} &= \frac{x_{i,y} - x_{i,y-1}}{1-x_{i,y-1}} \\ m_{i,y} &= \begin{cases} 1 & \text{if } u_i < p_{i,y} \text{ or } m_{i,y-1} = 1 \\ 0 & \text{if } u_i > p_{i,y} \end{cases} \end{aligned} \quad \text{App. Equation 7a, b, c}$$

104

105  $W_{i,y} = 1.35 \times 10^{-6} L_{i,y}^{3.42}$  App. Equation 8

106  
107  $SSB_y = \sum_1^i S_{i,y} W_{i,y} m_{i,y}$  App. Equation 9

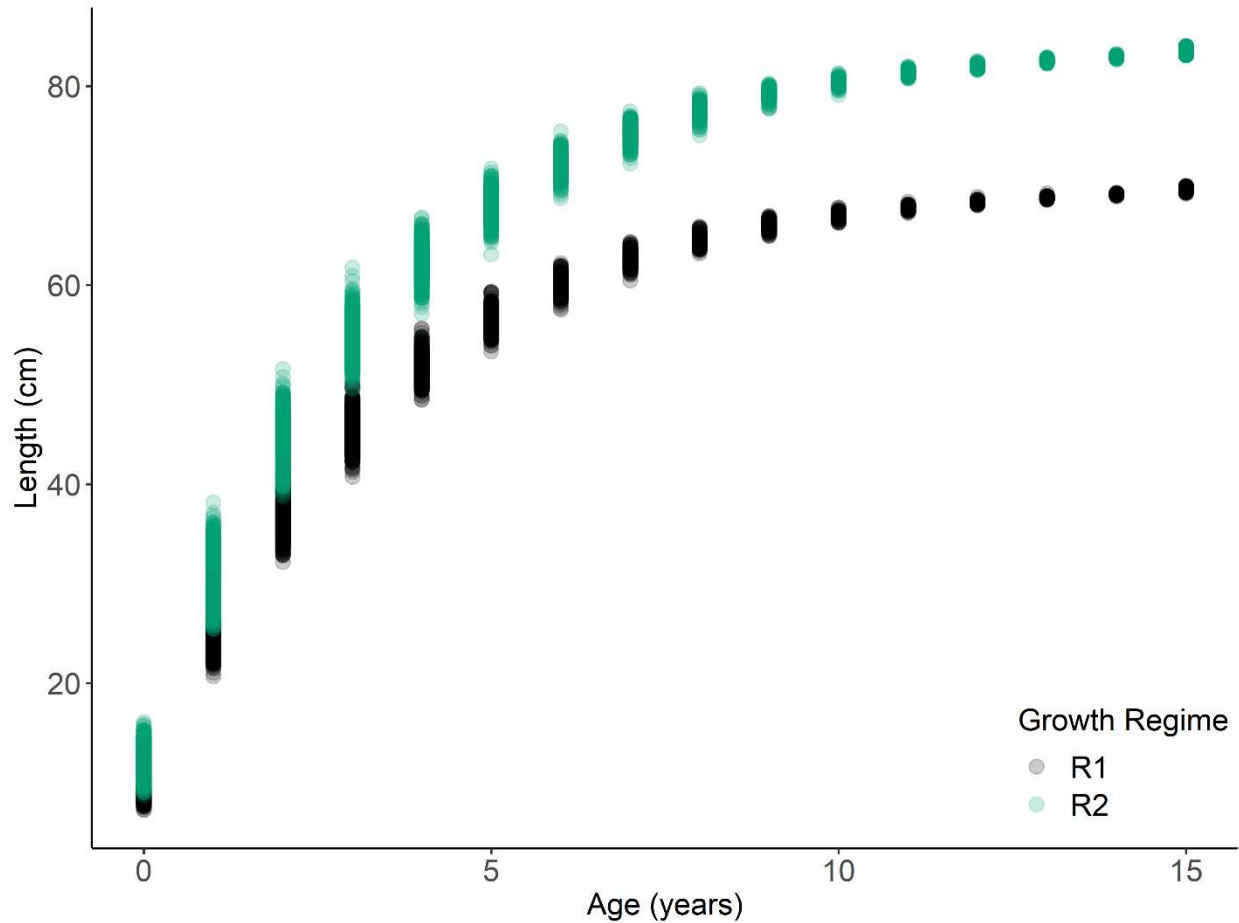
108  
109  $R_y = \frac{4h}{SSB_0(1-h)+SSB_{y-1}(5h-1)} \exp(\partial_{r,y})$  App. Equation 10

110  
111  $\partial_{r,y} = N(0, \sigma_r) - 0.5\sigma_r^2$  App. Equation 11

112 *A.1.4 Assigning spatio-temporal variation to synthetic populations*

113 The simulation testing component required generation of datasets that comprised variation in fish length-at-  
 114 age across space and/or time. To obtain spatial variation in length-at-age, we conducted simulations using one  
 115 of two growth “regimes”. Our synthetic populations were designed to mimic the level of variation among  $L_1$   
 116 and  $L_2$  in the sablefish dataset, which ranged from 10% to 40% between regions (see main text, Table 3 and  
 117 Figure 8); we used a slightly conservative difference in 20% for each of  $L_1$  and  $L_2$  to generate our synthetic  
 118 population. Other parameters were held constant across regimes. Spatial scenarios tested are described in  
 119 Table 1 of the main text. To simulate spatial zones, fish locations were sampled from a uniform distribution  
 120 with boundaries specific to a certain growth regime. In all except Scenario 4, where the break is located at 48°  
 121 and non-spatial scenarios, the latitude and longitude of fish grown under regime 1 were sampled  
 122 independently and at random from a uniform distribution between 0° and 25°; for simulations with spatial  
 123 variation, fish grown under regime 2 have latitude and longitude sampled uniformly from 25° to 50°. In  
 124 Scenario 4, all simulated fish were assigned latitudes sampled independently and at random from a uniform  
 125 distribution from 0° to 50°. Fish simulated under regime 2 were assigned longitudes sampled randomly from  
 126 0° to 48° and fish simulated under regime 2 have longitudes sampled randomly from 48° to 50°, forming a  
 127 vertical “band” of larger fish in higher longitudes.

128  
129



130  
131

132 Figure A2. Example growth trajectories from simulated populations. Each circle represents a simulated  
133 individual fish's length and age; colors correspond to the growth regime (i.e., growth curve) under which that  
134 fish was generated.

| Module      | Parameter            | Definition  | Value                              |
|-------------|----------------------|---|------------------------------------|
| Growth      | $L_1$                | Length at age $a_1$ (cm)                                  | 10 (regime 1)<br>70 (regime 2)     |
|             | $L_2$                | Length at age $a_2$ (cm)                                  | 12 (regime 1)<br>84 (regime 2)     |
| Growth      | $k$                  | Growth coefficient ( $\text{year}^{-1}$ )                 | 0.30 (regime 1)<br>0.30 (regime 2) |
|             | $a_1$                | Age at $L_1$ (years)                                      | 3                                  |
| Growth      | $a_2$                | Age at $L_2$ (years)                                      | 30                                 |
| Growth      | $\sigma_\varepsilon$ | Lognormal growth error term                               | 0.1                                |
| Growth      | $a$                  | Multiplier of length-weight function<br>( $\text{g/cm}$ ) | 1.35e-6                            |
| Growth      | $b$                  | Exponent of length-weight function                        | 3.427                              |
| Survival    | $M$                  | Natural mortality ( $\text{yr}^{-1}$ )                    | 0.25                               |
| Recruitment | $r$                  | Slope of maturity ogive                                   | -0.1034                            |
| Recruitment | $L_{50}$             | Length at 50% maturity (cm)                               | 44                                 |
| Recruitment | $h$                  | Steepness of Beverton-Holt SRR                            | 0.9                                |
| Recruitment | $R_0$                | Maximum number of recruits per year                       | 12                                 |
| Recruitment | $\sigma_r$           | Variation in recruitment                                  | 0.1                                |

Table A1. Parameter symbols, definitions and values used in the simulation study.

|                 |   |  | Original sample size<br>(average # age six fish = 530)   |  | With sample size halved                                  |  | With sample size reduced by 25%                          |  |
|-----------------|---|--|--|--|--|--|--|--|
| Scenario Number | Scenario Description  | True Break Points  | Coverage probability for L <sub>1</sub> , L <sub>2</sub> | Proportion correct latitude, longitude, year | Coverage probability for L <sub>1</sub> , L <sub>2</sub> | Proportion correct latitude, longitude, year | Coverage probability for L <sub>1</sub> , L <sub>2</sub> | Proportion correct latitude, longitude, year |
| 1               | No spatial breaks   | None   | 0.96, 0.74   | 0.86, 0.86, 0.82                             | 0.96, 0.02   | 0.95, 0.93, 0.75                             | 0.95, 0.01   | 0.95, 0.91, 0.83                             |
| 2               | Single, spatial break in middle of range, with no overlap and strong contrast | 25° Latitude and 25° Longitude   | 0.48, 0.43   | 0.92, 0.99, 0.89                             | 0.47, 0.02   | 0.78, 0.8, 0.87                              | 0.48, 0  | 0.82, 0.92, 0.86                             |
| 3               | Some overlap between regions  | Between 20° and 25° Latitude   | 0.85, 0.58   | 0.84, 0.11, 0.91                             | 0.86, 0  | 0.75, 0.21, 0.8                              | 0.87, 0  | 0.79, 0.14, 0.88                             |
| 4               | Single spatial break at edge of range with no overlap                         | 48° Longitude  | 0.27, 0.16   | 1, 1, 0.85                                   | 0.3, 0.02  | 0.99, 0.97, 0.92                             | 0.29, 0.02   | 0.99, 0.97, 0.79                             |
| 5               | Single temporal break at year 50 (of 100); no spatial variability             | None for latitude or longitude; all fish under regime 1 from years 0 to 49 and regime 2 thereafter | 0.97, 0.78   | 0.92, 0.96, 0.5                              | 0.9, 0.13  | 0.95, 0.96, 0.25                             | 0.95, 0.08   | 0.92, 0.96, 0.33                             |

137 Table A2. Summary of true break points, coverage probabilities of the endpoints of the post-aggregation  
138 growth curves, and the proportion of simulations which detected the exact breakpoints each or all of the three  
139 smoothers. For the overlapping scenario (Scenario 3), spatial breakpoints were considered a match if they fell  
140 within the true range. This analysis was repeated for the same datasets with the number of age-six fish reduced  
141 by either 50% or 25%.

## 142 A.2 – Additional tables and figures from the GAM-based analysis of sablefish size at age.

143

| Age | Sex | n    |
|-----|-----|------|
| 4   | F   | 4366 |
| 4   | M   | 3204 |
| 6   | F   | 4413 |
| 6   | M   | 3404 |
| 10  | F   | 2064 |
| 10  | M   | 1765 |
| 30  | F   | 168  |
| 30  | M   | 231  |

144

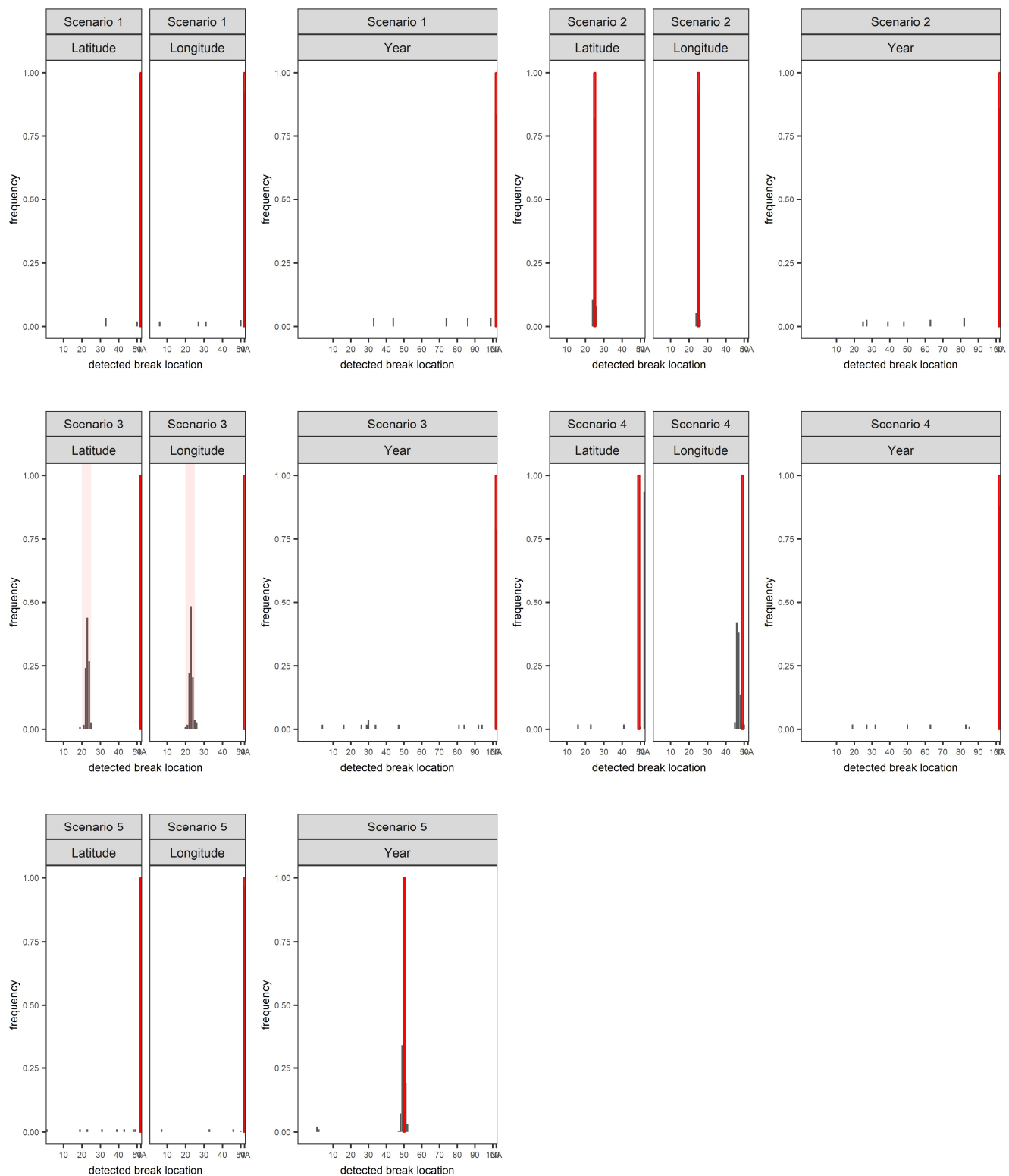
145 Table A3. Number of sablefish at key ages by sex and used in VBGF estimation for application study.

146

| Scenario Number | Scenario Description  | Year accurately detected | Mean absolute error in $L_2$ (cm) |
|-----------------|---|--------------------------|-----------------------------------|
| 1               | No spatial breaks   | FALSE                    | 0.403857                          |
| 1               | No spatial breaks   | TRUE                     | 0.464984                          |
| 2               | Single, spatial break in middle of range, with no overlap         | FALSE                    | 7.019933                          |
| 2               | Single, spatial break in middle of range, with no overlap         | TRUE                     | 6.975099                          |
| 4               | Single spatial break at edge of range with no overlap             | FALSE                    | 0.95649                           |
| 4               | Single spatial break at edge of range with no overlap             | TRUE                     | 1.165541                          |
| 3               | Some overlap between regions                                      | FALSE                    | 7.031669                          |
| 3               | Some overlap between regions                                      | TRUE                     | 6.415294                          |
| 5               | Single temporal break at year 50 (of 100); no spatial variability | FALSE                    | 0.668129                          |
| 5               | Single temporal break at year 50 (of 100); no spatial variability | TRUE                     | 0.463615                          |

147

148 Table A4. Mean absolute error in estimated  $L_2$  across simulated scenarios with a 95% CI for  $L_2$  which did not  
149 contain the true value, depending on whether the temporal breakpoint was accurately detected (TRUE or  
150 FALSE). Average Error is computed as the mean of the absolute difference between the end of the estimated  
151 confidence interval and the true value; if the true value was higher than the confidence interval, the difference  
152 is measured from the upper end of the interval and vice versa.



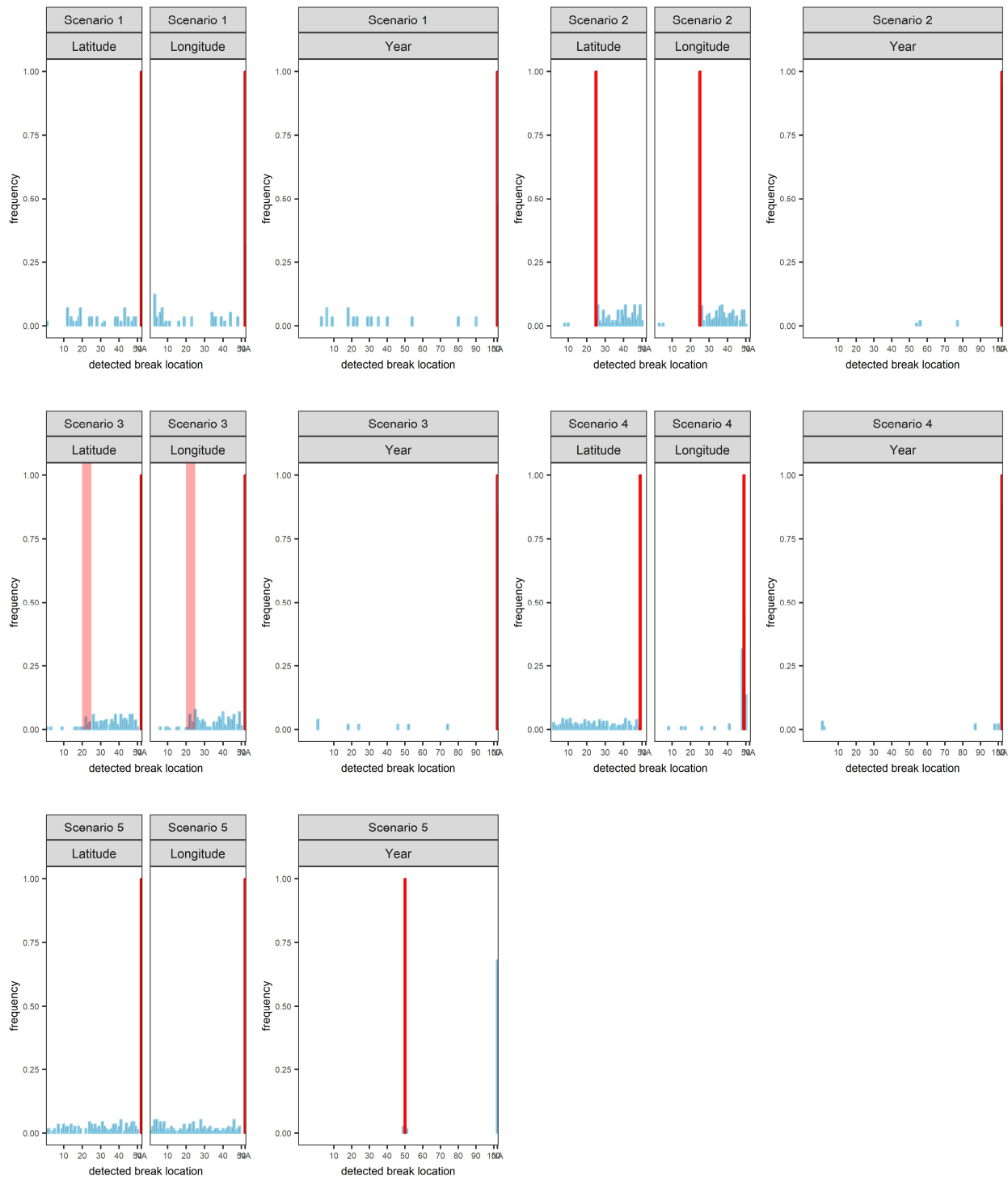
153

154

155

156

Figure A3 Histogram of detected breakpoints (grey bars) from the GAM analysis by scenario. Vertical red bars indicate true breakpoints used to generate synthetic populations. For Scenario 3, the synthetic population overlapped between 20 and 25 degrees latitude and longitude.



157  
158  
159  
160

Figure A4 Histogram of detected breakpoints (grey bars) from the STARS analysis by scenario. Vertical red bars indicate true breakpoints used to generate synthetic populations. For Scenario 3, the synthetic population overlapped between 20 and 25 degrees latitude and longitude.

Figure A6 through Figure A15 are identical in form to Figure 5 and 6 in main text, which presented results for age six female sablefish. These plots contain results for ages four and thirty for males and females, and age-four males.

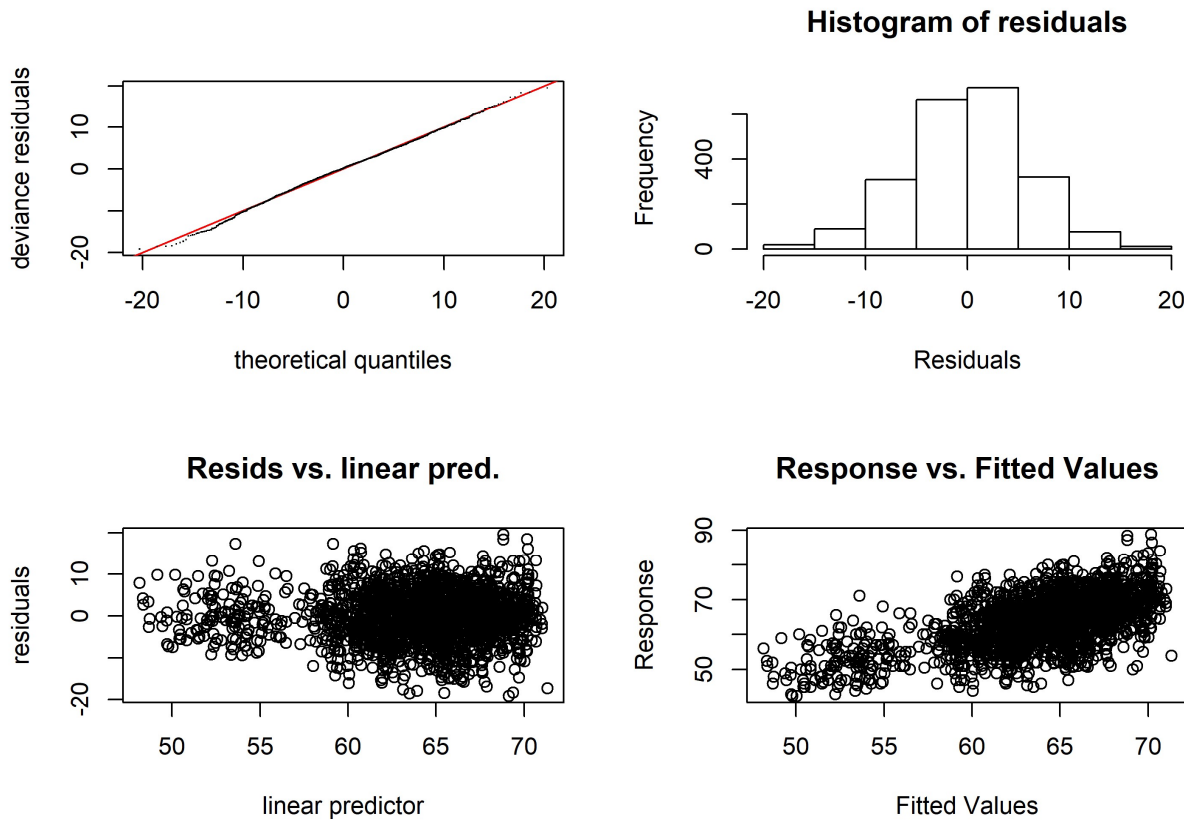
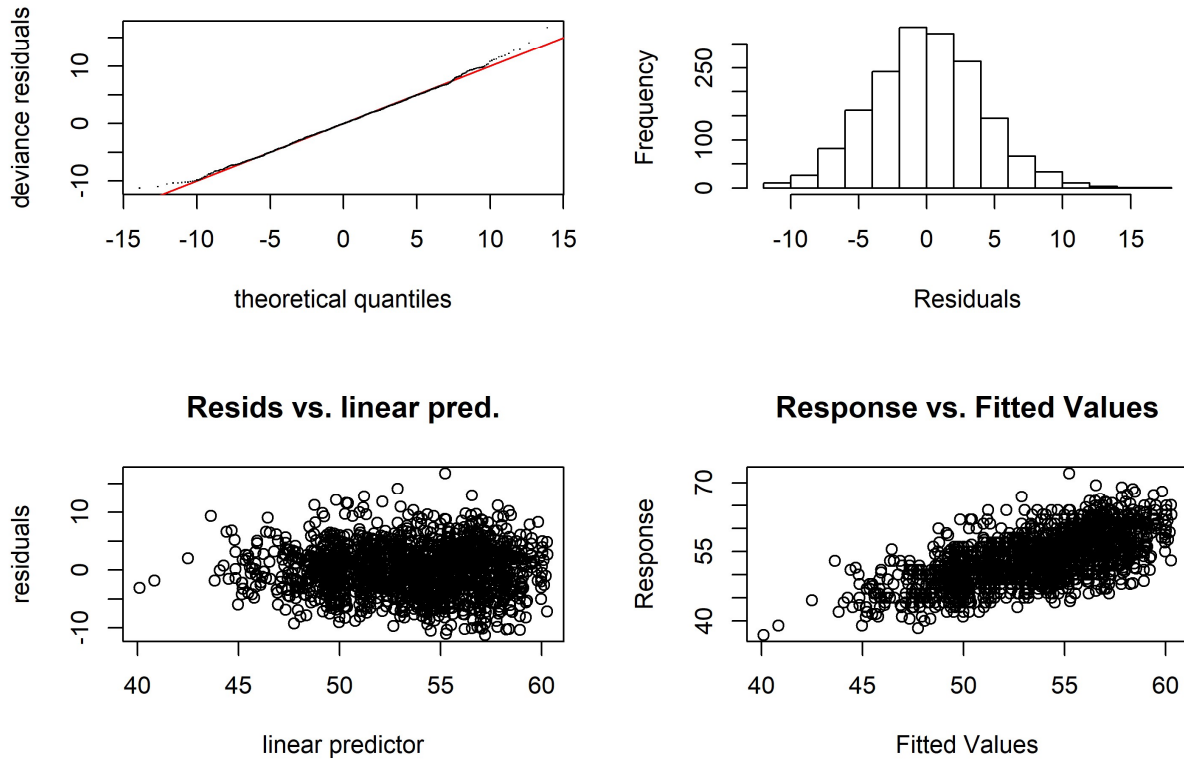
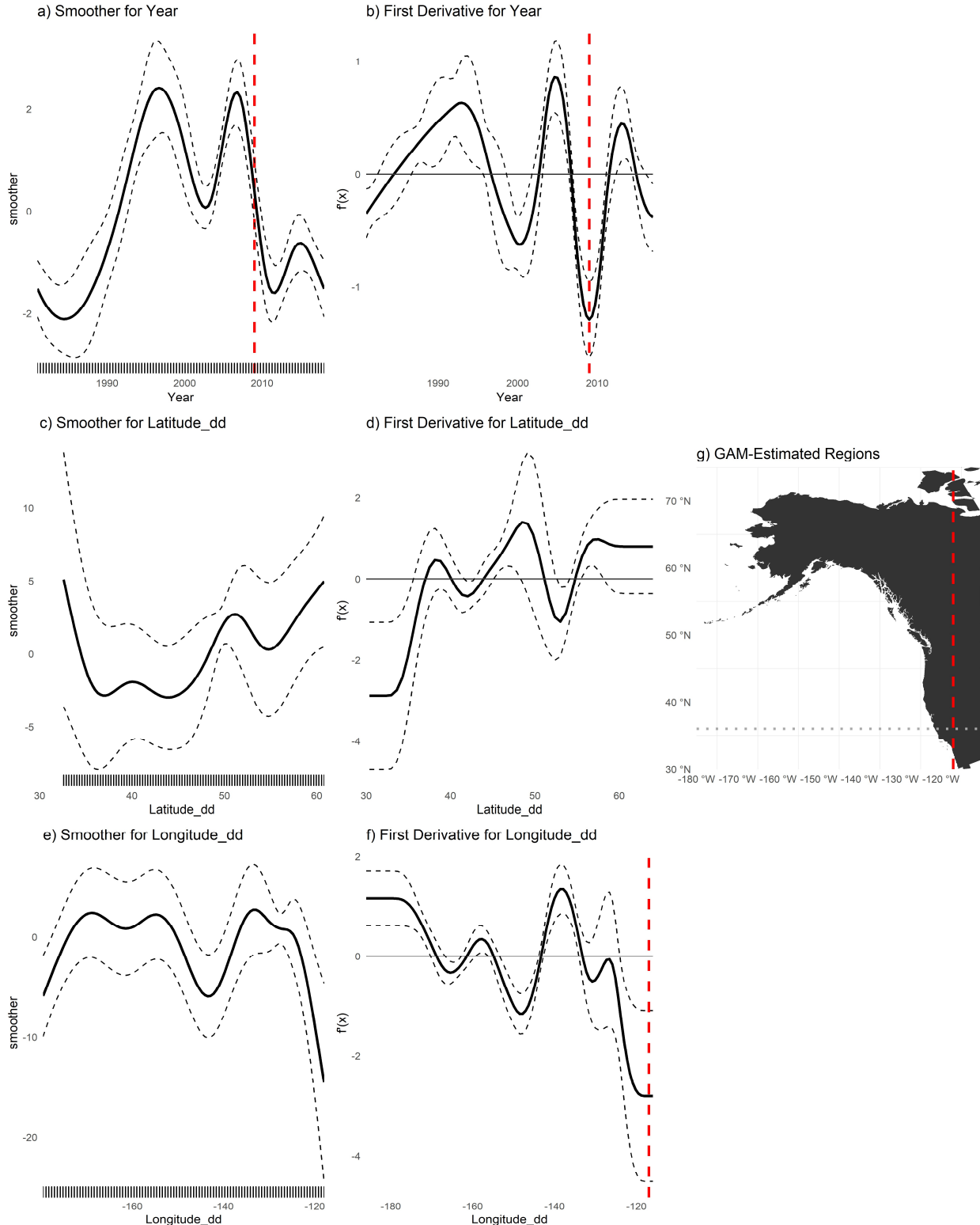


Figure A5. Diagnostic plots of best-fit GAM model for female age four sablefish. Clockwise from top left: quantile-quantile plot of deviance residuals; histogram of residuals; observed response values (lengths, in cm) vs predicted values, and model-predicted residuals vs linear predictor. See Supplementary Material for equivalent plots for other key ages and all sexes.

1  
2  
3  
4

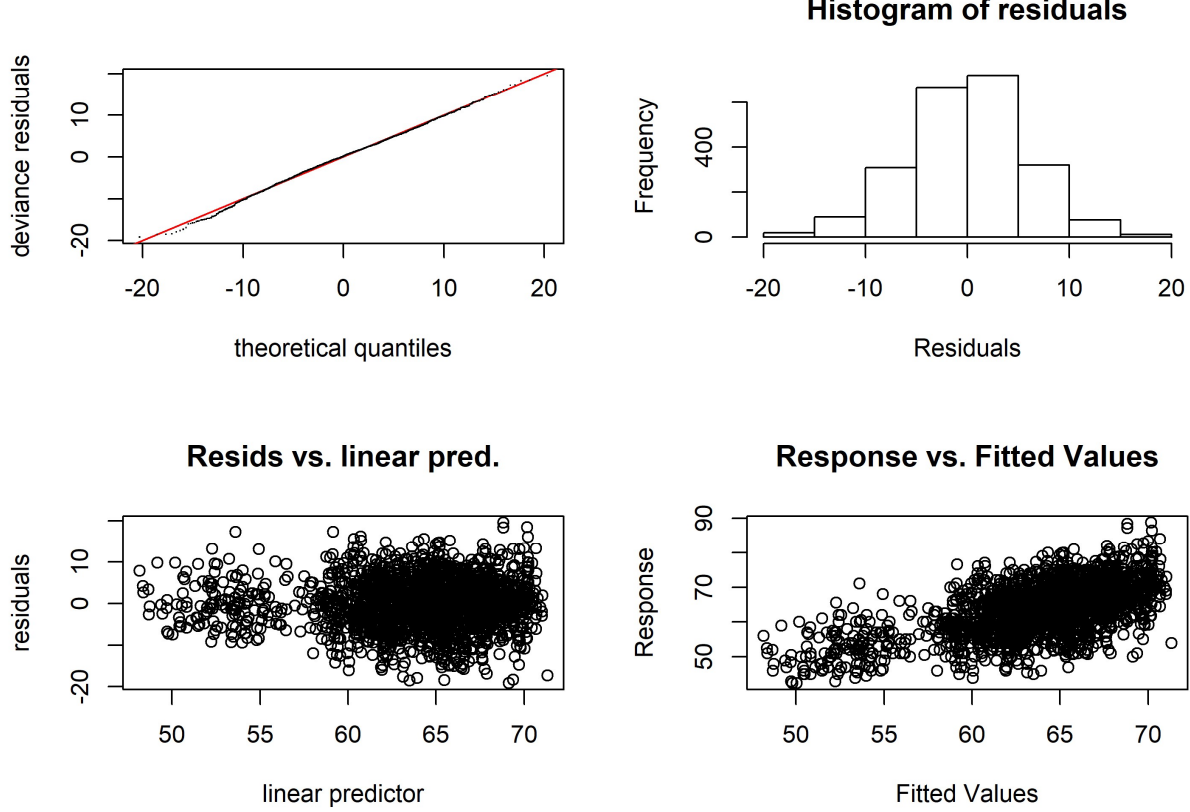


5  
6 Figure A6 Diagnostic plots of best-fit GAM model for male age four sablefish. Clockwise from top left:  
7 quantile-quantile plot of deviance residuals; histogram of residuals; observed response values (lengths, in  
8 cm) vs predicted values, and model-predicted residuals vs linear predictor.

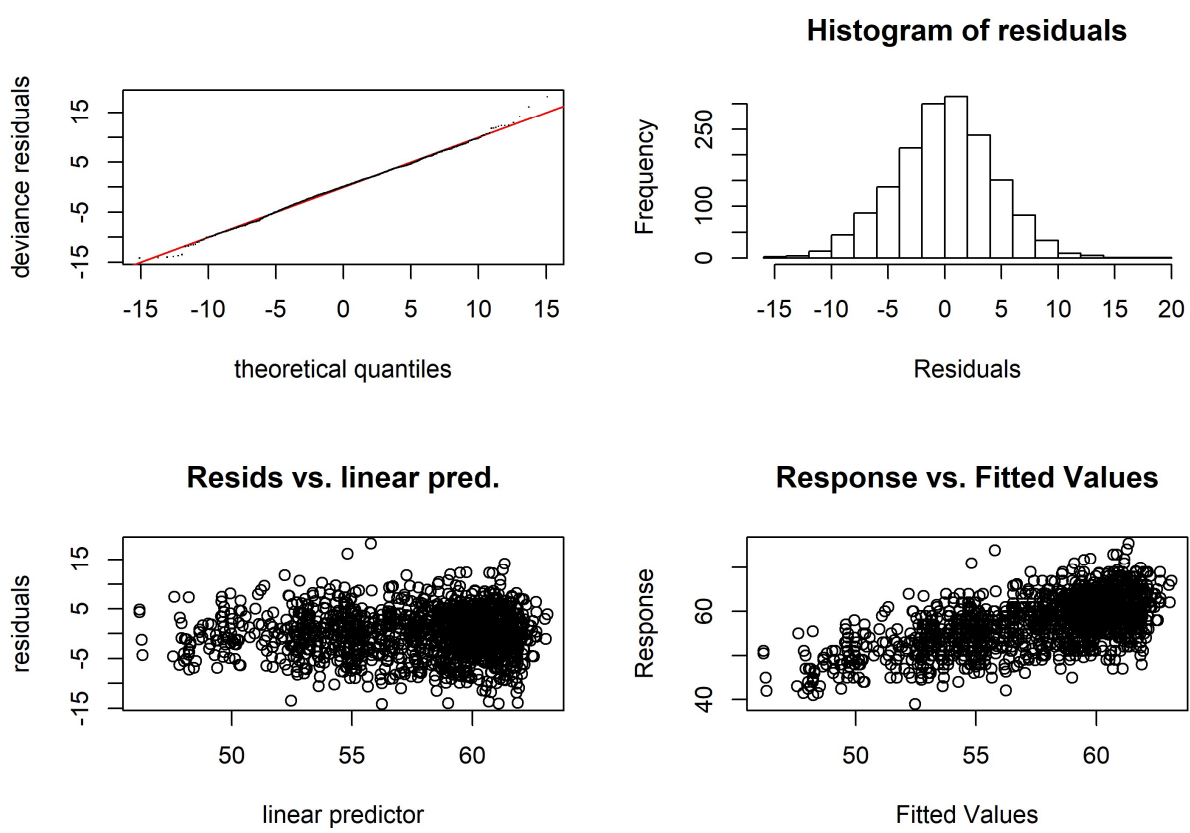


9

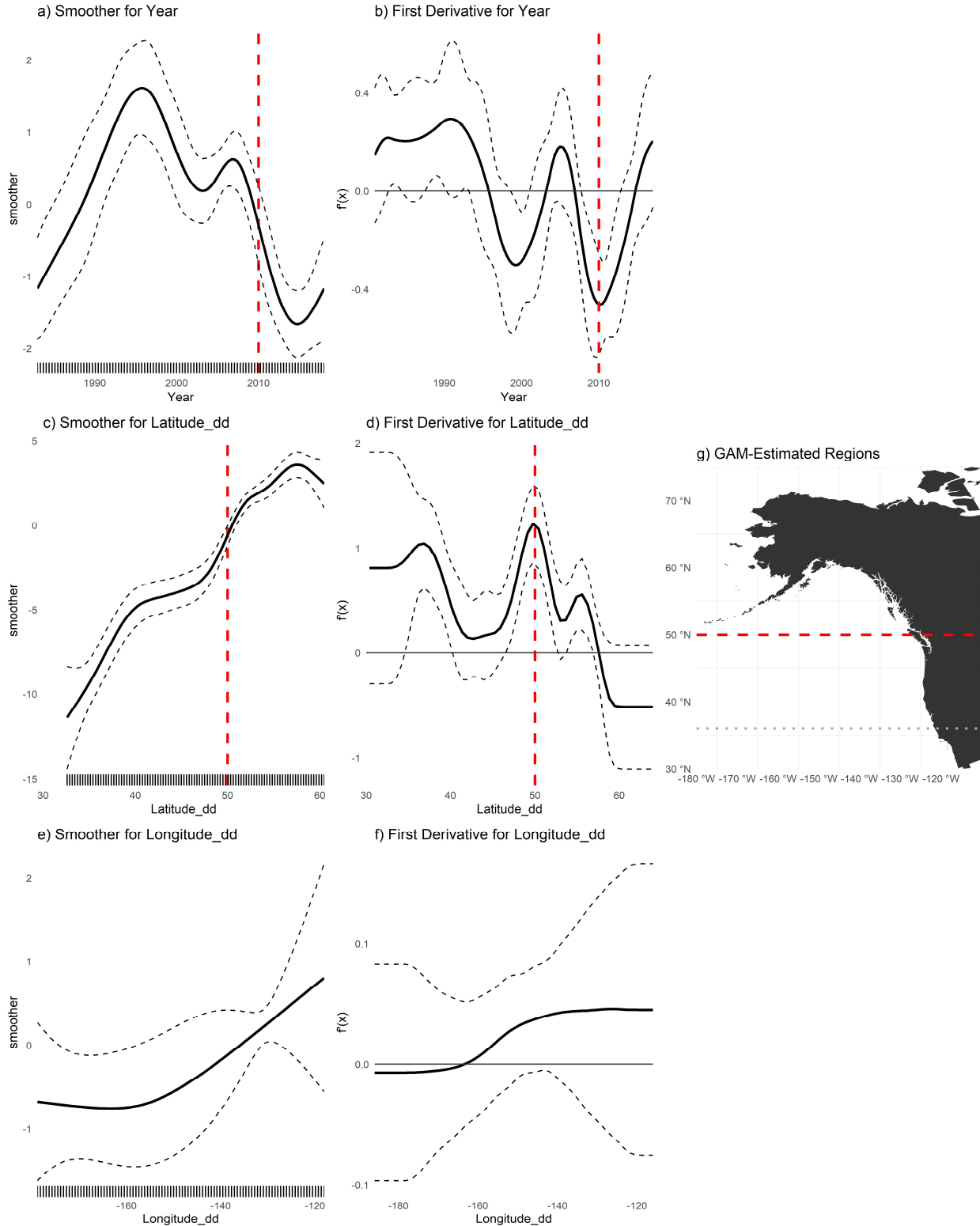
10 Figure A7 (a,c,e) Plots of smoothers for Year, Latitude, and Longitude, and first derivatives thereof for age-  
 11 four male sablefish (b,d,f). Red lines indicate latitudes or longitudes that produced the highest first derivative  
 12 and had a confidence interval that did not include zero. g) map with model-detected breakpoints (red lines).



13  
14 Figure A8 Diagnostic plots of best-fit GAM model for female age six sablefish. Clockwise from top left:  
15 quantile-quantile plot of deviance residuals; histogram of residuals; observed response values (lengths, in  
16 cm) vs predicted values, and model-predicted residuals vs linear predictor.



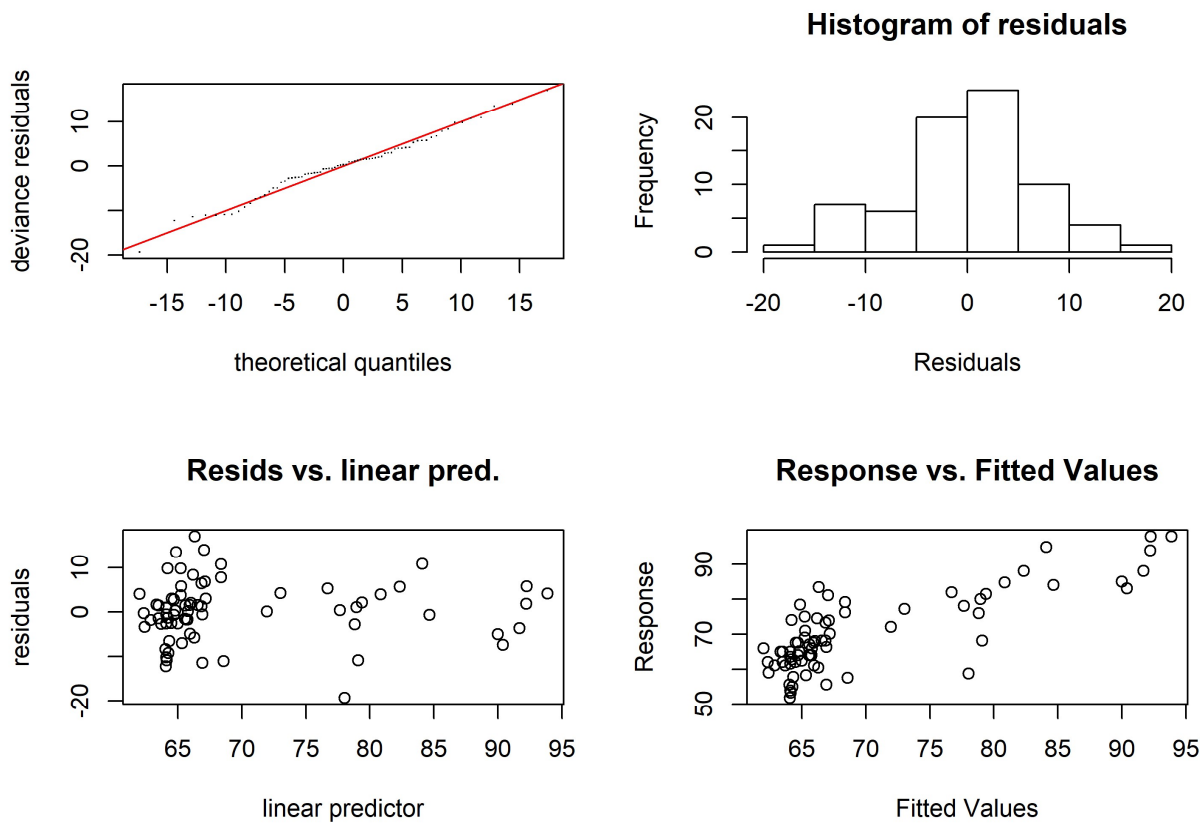
17  
18 Figure A9 Diagnostic plots of best-fit GAM model for male age six sablefish. Clockwise from top left:  
19 quantile-quantile plot of deviance residuals; histogram of residuals; observed response values (lengths, in  
20 cm) vs predicted values, and model-predicted residuals vs linear predictor.



21

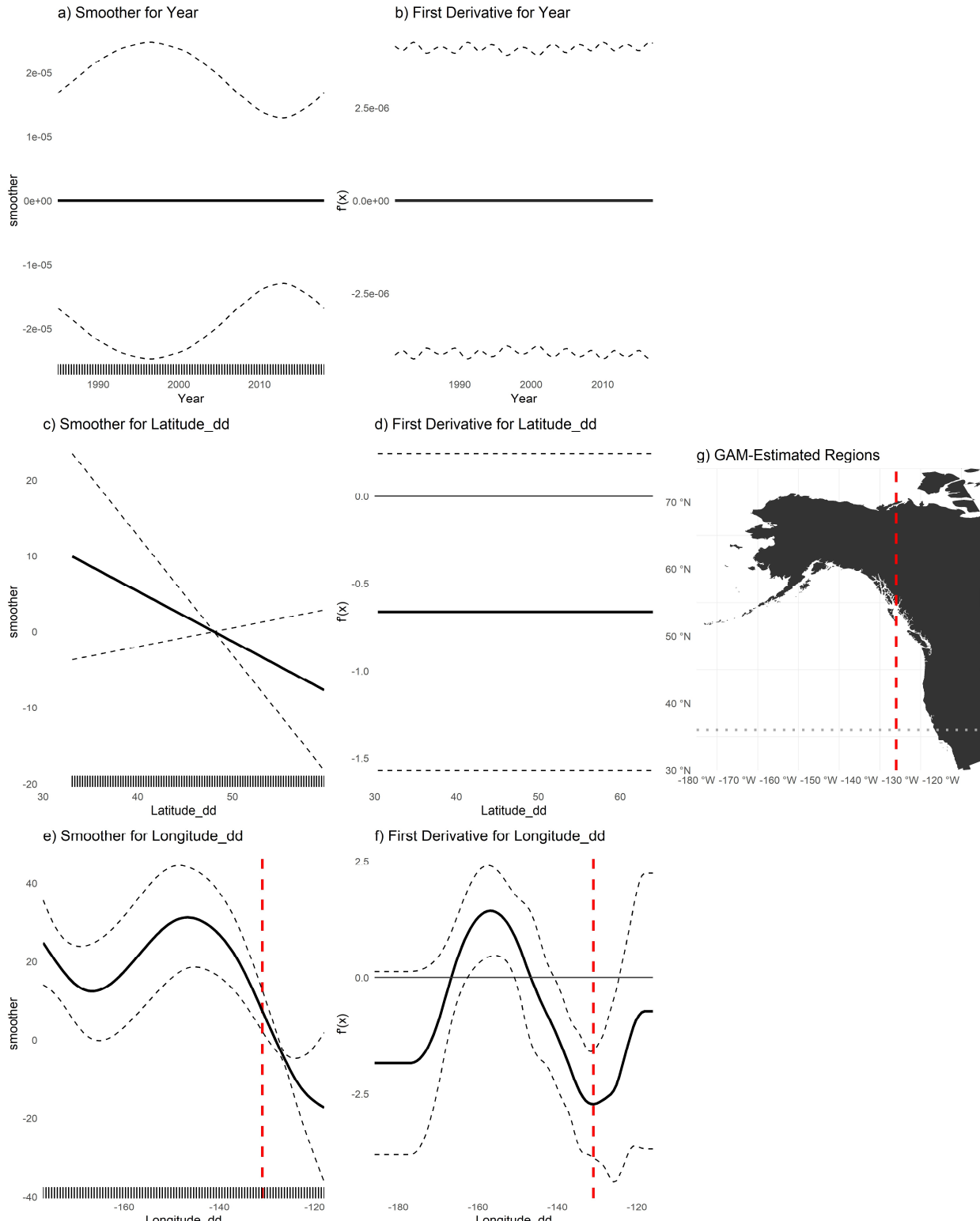
22 Figure A10 (a,c,e) Plots of smoothers for Year, Latitude, and Longitude, and first  
 23 derivatives thereof for male age six sablefish (b,d,f). Red lines indicate latitudes or longitudes that produced the highest first  
 24 derivative and had a confidence interval that did not include zero.g) map with model-detected breakpoints  
 25 (red lines).

26



27

28 Figure A11 Diagnostic plots of best-fit GAM model for female age thirty sablefish. Clockwise from top left:  
29 quantile-quantile plot of deviance residuals; histogram of residuals; observed response values (lengths, in  
30 cm) vs predicted values, and model-predicted residuals vs linear predictor.

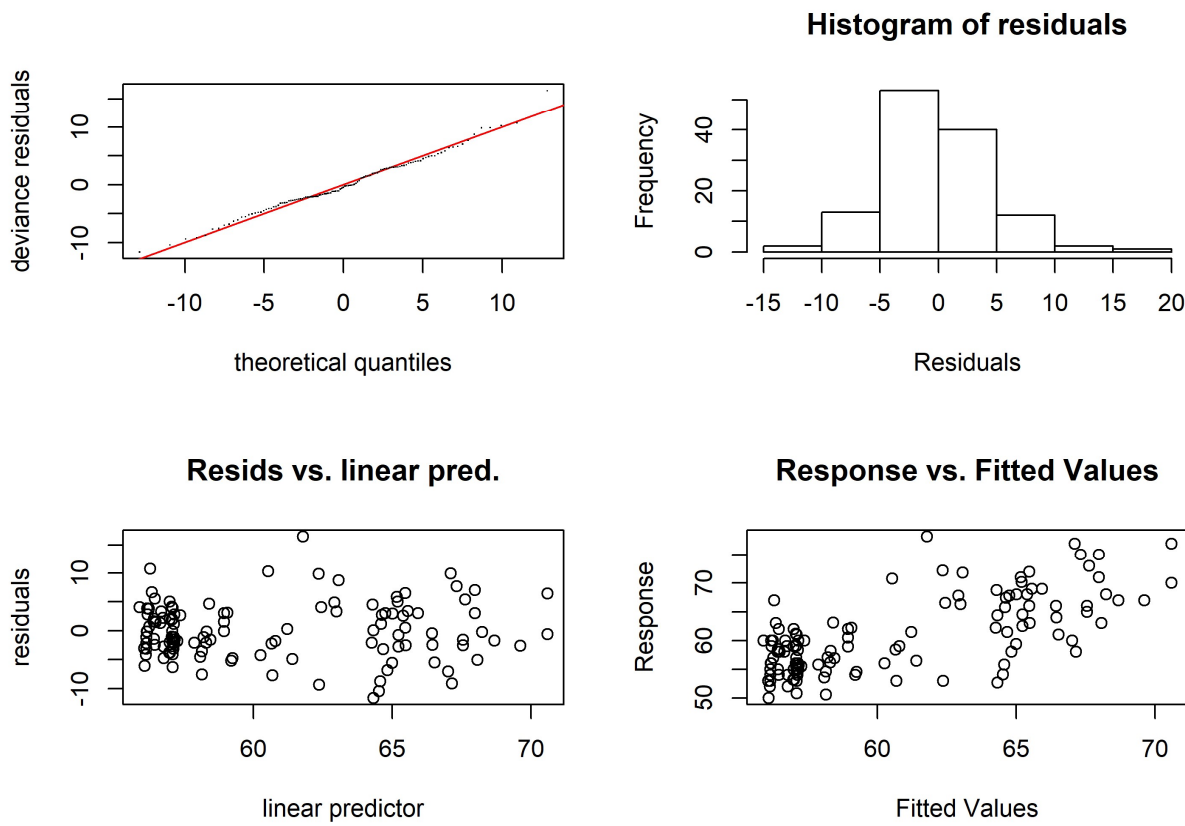


31

32

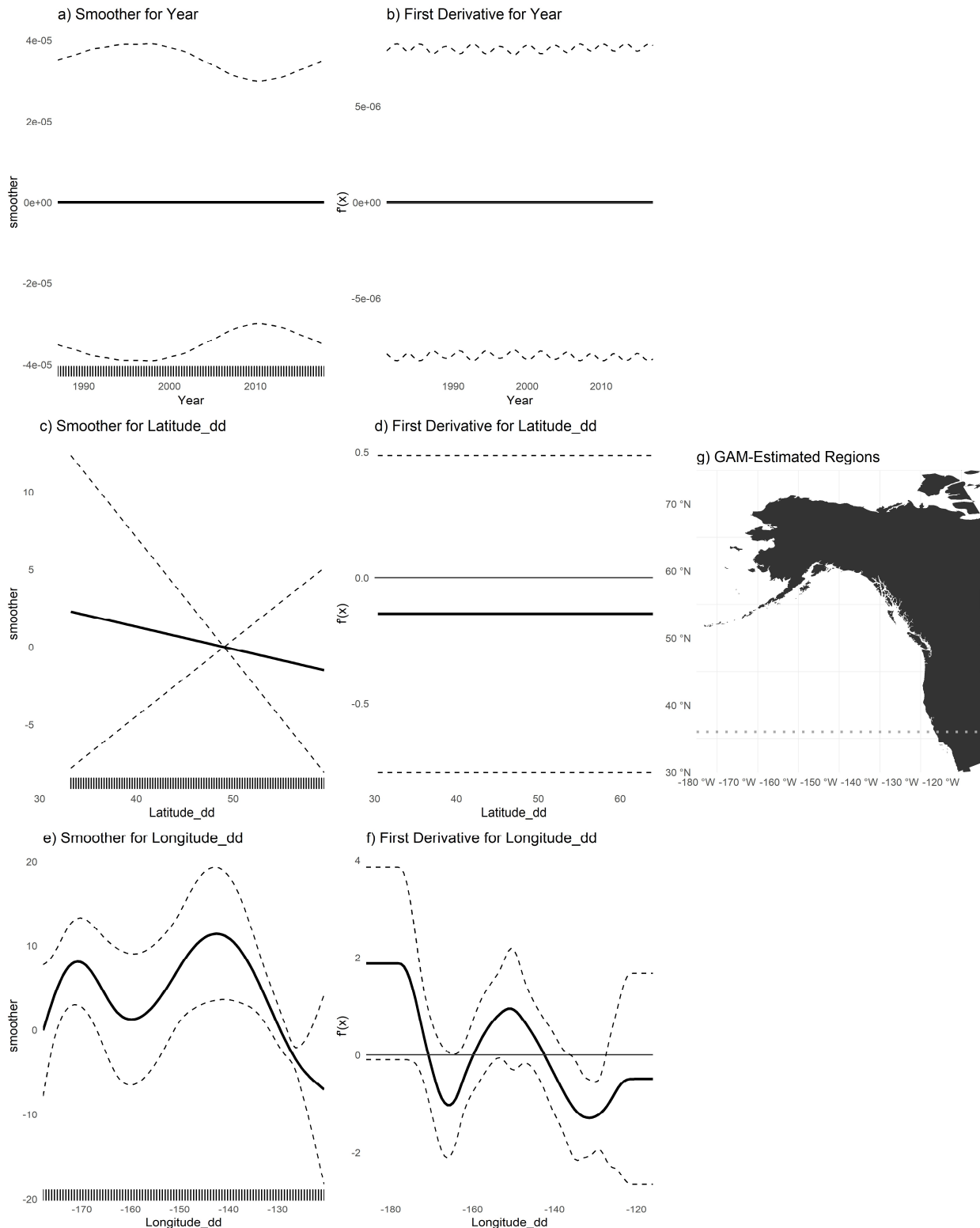
Figure A12 (a,c,e) Plots of smoothers for Year, Latitude, and Longitude, and first derivatives thereof for female age thirty sablefish (b,d,f). Red lines indicate latitudes or longitudes that produced the highest first derivative and had a confidence interval that did not include zero. g) map with model-detected breakpoints (red lines).

36



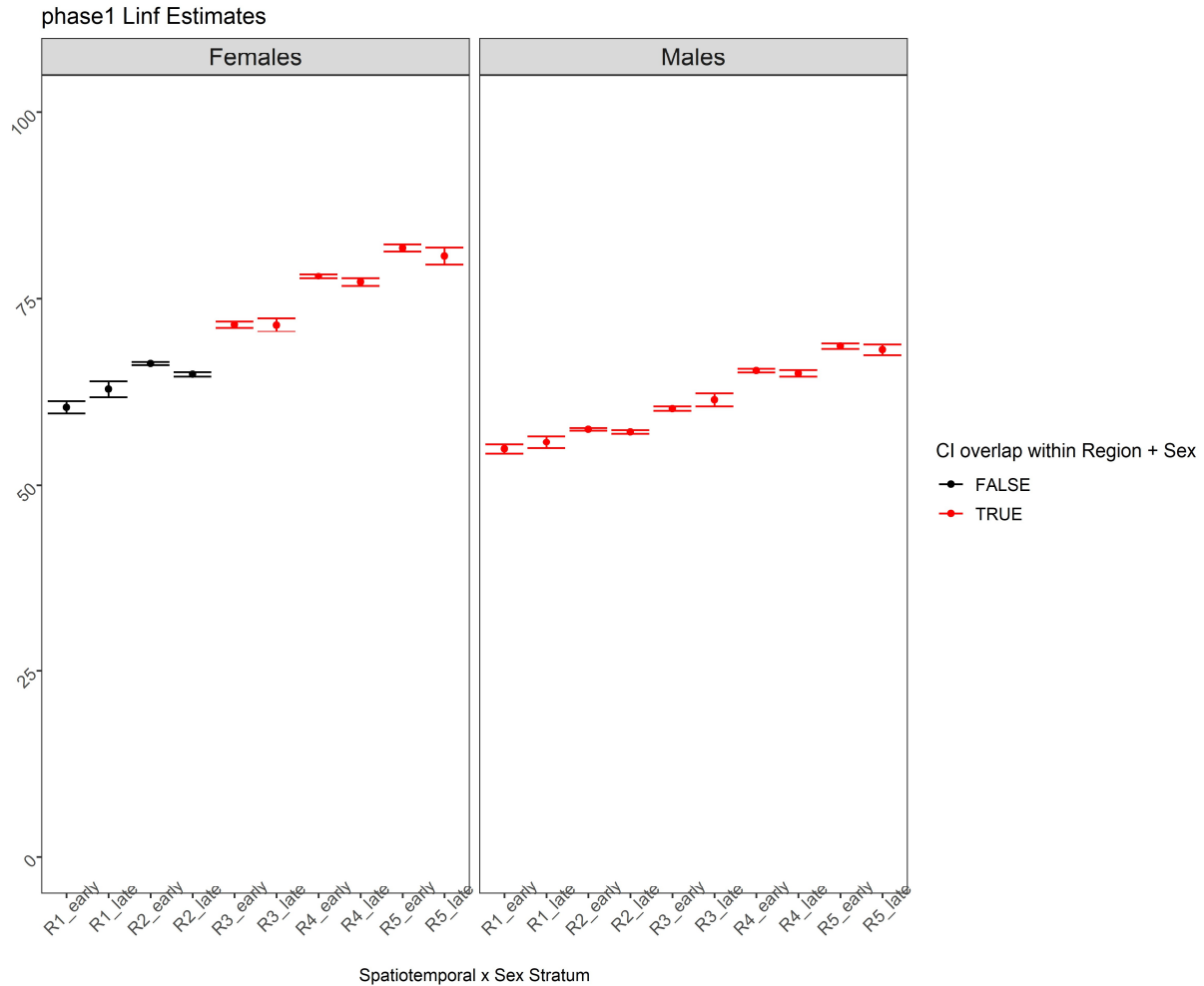
37

38 Figure A13 Diagnostic plots of best-fit GAM model for male age thirty sablefish. Clockwise from top left:  
39 quantile-quantile plot of deviance residuals; histogram of residuals; observed response values (lengths, in  
40 cm) vs predicted values, and model-predicted residuals vs linear predictor.  
41

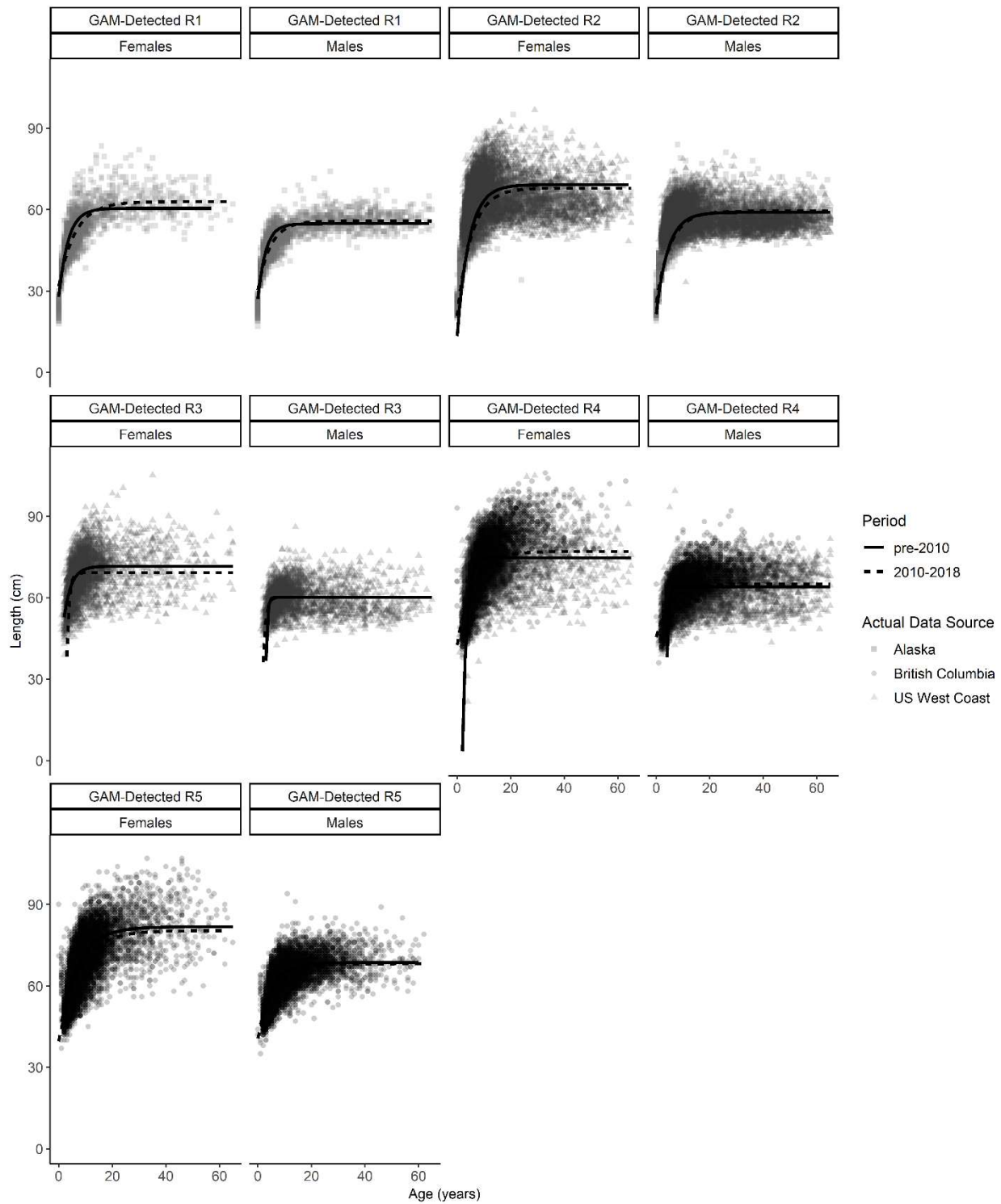


42

43 Figure A14 (a,c,e) Plots of smoothers for Year, Latitude, and Longitude, and first  
 44 derivatives thereof for male age thirty sablefish (b,d,f). Red lines indicate latitudes or longitudes that produced the highest first  
 45 derivative and had a confidence interval that did not include zero. g) map with model-detected breakpoints  
 46 (red lines).



47  
48 Figure A15  $L_\infty$  estimates for the fully stratified, 5-region, 2-period (during and after 2010, and before) and 2-  
49 sex model. Bars represent 95% confidence intervals. Strata from the same spatial region and sex that shared  
50 overlapping ranges for  $L_\infty$  are colored in red and early and late periods were combined within their  
51 respective regions and sexes for the subsequent analysis.





- 57      *References*
- 58      Beverton, R.J.H., Holt, S.J., 1957. On the Dynamics of Exploited Fish Populations, Fisheries Investigations  
59              Series 2: Sea Fisheries. <https://doi.org/10.1007/BF00044132>
- 60      Kirkwood, G.P., 1983. Estimation of von Bertalanffy Growth Curve Parameters Using both Length  
61              Increment and Age-Length Data. *Can. J. Fish. Aquat. Sci.* 40, 1405–1411.  
62              <https://doi.org/10.1139/f83-162>
- 63      Rodionov, S.N., 2004. A sequential algorithm for testing climate regime shifts. *Geophys. Res. Lett.* 31, 2–5.  
64              <https://doi.org/10.1029/2004GL019448>
- 65